OXFORD UNIVERSITY PRESS | Human Molecular Genetics

The Pro-Apoptotic JNK Scaffold POSH/SH3RF1 Mediates *CHMP2B*^{Intron5}-Associated Toxicity in Animal Models Frontotemporal Dementia

Journal:	*Human Molecular Genetics*
Manuscript ID	HMG-2017-D-01148.R1
Manuscript Type:	2 General Article - UK Office
Date Submitted by the Author:	02-Feb-2018
Complete List of Authors:	West, Ryan; University of York, Biology Ugbode, Chris; University of York, Department of Biology Gao, Fen-Biao; University of Massachusetts, Neurology Sweeney, Sean; University of York, Department of Biology
Key Words:	Frontotemporal Dementia, Drosophila, POSH, CHMP2B

The Pro-Apoptotic JNK Scaffold POSH/SH3RF1 Mediates *CHMP2B*^{Intron5}-Associated Toxicity in Animal Models of Frontotemporal Dementia

Ryan J. H. West [1], Chris Ugbode [1], Fen-Biao Gao [2], Sean T. Sweeney [1,*]

Affiliations:

[1] Department of Biology, University of York, York, YO10 5DD, UK

[2] Department of Neurology, University of Massachusetts Medical School, Worcester, MA 01605

*To whom correspondence should be addressed at: Department of Biology and Hull-York Medical School, University of York, Wentworth Way, Heslington, York YO10 5YW, UK. Tel: +44-1904-328537; Fax: +44-1904-328505; Email: sean.sweeney@york.ac.uk

Abstract

Frontotemporal Dementia (FTD) is one of the most prevalent forms of early-onset dementia. However, the pathological mechanisms driving neuronal atrophy in FTD remain poorly understood. Here we identify a conserved role for the novel pro-apoptotic protein POSH/SH3RF1 in mediating neuropathology in *Drosophila* and mammalian models of *CHMP2B*^{Intron5} associated FTD. Aberrant, AKT dependent, accumulation of POSH was observed throughout the nervous system of both *Drosophila* and mice expressing *CHMP2B*^{Intron5}. Knockdown of POSH was shown to be neuroprotective and sufficient to alleviate aberrant neuronal morphology, behavioral deficits and premature-lethality in *Drosophila* models, as well as dendritic collapse and cell death in *CHMP2B*^{Intron5} expressing rat primary neurons. POSH knockdown also ameliorated elevated markers of JNK and apoptotic cascades in both *Drosophila* and mammalian models. This study provides the first characterization of POSH as a potential component of an FTD neuropathology, identifying a novel apoptotic pathway with relevance to the FTD spectrum.

Introduction

Frontotemporal Dementia (FTD), a clinically, genetically and pathologically heterogeneous neurodegenerative disease, is a common form of early-onset dementia. FTD refers to a group of clinical syndromes associated with Frontotemporal lobar degeneration (FTLD), a progressive degeneration of the frontal and temporal lobes of the brain. The principal syndromes associated with FTLD include behavioral variant FTD (bvFTD), progressive non-fluent aphasia, semantic dementia and FTD with Motor Neuron Disease (FTD-MND). bvFTD is the most prevalent, accounting for ~ 60% of all FTD cases. Perturbed regulation of apoptosis is a proposed mechanism underpinning neuronal death in FTD and has been observed in different FTD variants(1-7). A number of FTD loci are implicated in neuronal apoptosis (VCP, TBK1, GRN), however the cellular machinery driving the pro-apoptotic signal has yet to be determined(8, 9).

Previously we established a *Drosophila* model of FTD associated with the bvFTD-disease causing mutation *CHMP2B*^{Intron5} *(7, 10, 11)*. *CHMP2B*^{Intron5} causes a C-terminal truncation of the CHMP2B protein and failure of CHMP2B to dissociate from the endosomal sorting complex required for transport III complex(12, 13). Using this model we demonstrated *CHMP2B*^{Intron5} perturbs normal endosomal and autophagic trafficking*(7, 10, 11)*. Neuronal loss through phagocytic clearance of apoptotic neurons has been observed in *CHMP2B*^{Intron5} models(14), however the mechanisms driving this process are not fully established. Previously we found the pro-apoptotic JNK scaffold Plenty of SH3's (POSH/SH3RF1) is activated in *Rab8* mutants(7), dominant enhancers of *CHMP2B*^{Intron5}. We now show POSH accumulates in the nervous system and mediates toxicity in *Drosophila* and mammalian models of *CHMP2B*^{Intron5}.

POSH forms a scaffold for a multi-protein complex involved in JNK and NF-κB dependent apoptosis(15-17). This complex assembles following apoptotic stimuli and stabilises through association with JNK components(18-22). This self-amplifying feedback loop leads to JNK-dependent apoptosis and cell death(22). POSH overexpression induces neuronal apoptosis while knockdown conveys neuroprotection against ischemia(16, 23, 24). AKT inhibits POSH dependent apoptosis by promoting disassembly of the pro-apoptotic POSH-JNK complex(18-20).

Using our *Drosophila* model of *CHMP2B*^{Intron5} dominant screens were performed, identifying loci modifying *CHMP2B*^{Intron5} toxicity(7, 10, 11). This identified the pro-survival gene AKT as a potent modifier of *CHMP2B*^{Intron5} toxicity. Having shown accumulation of POSH to mediate neuronal dysfunction in *Rab8* mutants(7), another dominant modifier of CHM2B^{Intron5}, this study looked to elucidate a role for POSH as a component of neuropathological and pro-apoptotic cascades in FTD. Using *Drosophila*, primary mammalian neurons and neuronal tissue from *CHMP2B*^{Intron5} expressing mice we demonstrate POSH to be a conserved component of pathology in *CHMP2B*^{Intron5} *models.* We show POSH accumulates in neurons and drives unregulated synaptic growth, behavioral dysfunction and early-lethality in flies. POSH knockdown ameliorated dendritic collapse in primary mammalian neurons expressing CHMP2B^{Intron5}. In keeping with the pro-apoptotic function of POSH we demonstrate expression of *CHMP2B*^{Intron5} results in elevated JNK and apoptotic markers, both of which can be alleviated by POSH knockdown. This study implicates POSH as an important component of toxicity in *CHMP2B*^{Intron5} FTD, defining a novel pathway potentially mediating toxicity and neuronal survival in FTD.

Results

A genetic screen in *Drosophila* identifies *AKT* as a dominant modifier of *CHMP2B*^{Intron5} toxicity

Expression of the disease-causing *CHMP2B*^{Intron5} mutant transgene in the *Drosophila* eye elicits a perturbed eye phenotype, described previously(7, 10, 11). This phenotype allowed us to screen ~ 80% of the *Drosophila* genome for dominant modifiers of *CHMP2B*^{Intron5} toxicity(7, 10, 11). Here we identify *AKT* as a dominant enhancer of toxicity, with *AKT* loss-of-function alleles *AKT*^{04226} and *AKT*^{3} and AKT knockdown, via RNAi, potentiating the *CHMP2B*^{Intron5} eye phenotype (Fig. 1a-b). The kinase-dead *AKT* allele *AKT*^{1} showed the most significant enhancement of the eye phenotype (Fig. 1a-b)(25).

We previously demonstrated pan-neuronal expression of *CHMP2B*^{Intron5} results in unregulated synaptic overgrowth at the *Drosophila* larval neuromuscular junction (NMJ)*(7)*. We therefore employed this model to establish whether expression of AKT could alleviate neuronal aberrations in larvae pan-neuronally (*nSyb*-Gal4) expressing *CHMP2B*^{Intron5}. Expression of AKT or constitutively active myristoylated AKT (myrAKT) was sufficient to alleviate synaptic overgrowth, reducing both elevated synaptic bouton number and NMJ length (Fig. 1c-e). Co-expression of UAS-mCD8-GFP with *CHMP2B*^{Intron5} showed no variance to *CHMP2B*^{Intron5} expression alone, indicating rescues were not the result of titrating Gal4. To provide a functional, behavioral readout of NMJ activity larval locomotor assays were employed. *CHMP2B*^{Intron5} expressing larvae displayed significantly reduced larval crawling velocity, compared to wild-types or controls (Fig. 1f). Co-expression of AKT or myrAKT with *CHMP2B*^{Intron5} was sufficient to partially rescue locomotor deficits, with the myrAKT providing the most significant rescue (Fig. 1f).

AKT Mediates Aggregation of The Pro-Apoptotic JNK Scaffold POSH

AKT exhibits anti-apoptotic activity in neurons through direct interaction and phosphorylation of POSH(18). Previously we demonstrated POSH accumulation in the nervous system of larvae mutant for *Rab8*, a dominant modifier of $CHMP2B^{Intron5}$ *(7)*. Rab8 also interacts with TBK1, Optineurin and C9orf72, known loci causing FTD and MND(26-28). We therefore asked whether POSH accumulation was also observed in the nervous system of larvae expressing $CHMP2B^{Intron5}$, in a manner phenocopying *Rab8* mutants. Pan-neuronal expression of $CHMP2B^{Intron5}$ resulted in aberrant accumulation of POSH in distinct puncta throughout the larval ventral nerve cord (VNC) (fig. 2a). Puncta were most frequently observed within the neuropil, mimicking *Rab8* mutants, which show POSH accumulations throughout their axons. Quantification revealed a significant increase in POSH accumulations in the VNC of $CHMP2B^{Intron5}$ expressing animals, compared to wild-type (Fig. 2b). Having observed pan-neuronal expression of $CHMP2B^{Intron5}$ perturbs synaptic structure and function at the *Drosophila* larval NMJ (Fig. 1c-f) we also asked whether $CHMP2B^{Intron5}$ expression within motor neurons, using the OK6-Gal4 Driver, induced aberrant accumulation of POSH. Motor neuronal expression of $CHMP2B^{Intron5}$ was sufficient to induce aberrant accumulation of POSH puncta throughout the neuropil region of the VNC (Fig. 2c).

POSH is a substrate of AKT *in vitro* and in cell culture, with phosphorylation of POSH by AKT negatively regulating assembly of the pro-apoptotic POSH complex(18). We therefore looked to ascertain whether this interaction occurred *in vivo* in the *Drosophila* nervous system and whether inhibition of AKT kinase function affected POSH accumulation. The *Drosophila* AKT^{1} mutant allele is characterized by a point mutation leading to a single amino-

acid change (F327I) within a highly conserved region of the kinase catalytic core domain(25). This mutation results in a complete loss of kinase activity and is considered a kinase-dead allele. POSH was shown to accumulate throughout the larval VNC of *AKT*^{1} kinase-dead flies in a manner phenocopying *CHMP2B*^{Intron5} (fig. 2d). No significant accumulation of POSH was observed in wild-type animals. Immunoblotting using the anti-Phospho-(Ser/Thr) Akt Substrate Antibody, which preferentially recognizes peptides phosphorylated by AKT, following immunoprecipitation of POSH from *Drosophila* lysates, confirmed POSH to be a direct substrate of AKT *in vivo*(18) (supplementary fig. 1a).

Having observed POSH accumulations in the nervous system of *AKT*^{1} kinase dead flies (Fig. 2d) and demonstrated expression of AKT to be sufficient to rescue synaptic overgrowth at the *Drosophila* larval NMJ in *CHMP2B*^{Intron5} expressing animals (Fig. 1c-e), we looked to ascertain whether AKT expression could alleviate aberrant accumulation of POSH in the nervous system of *CHMP2B*^{Intron5} flies. Expression of AKT was sufficient to reduce the number of distinct POSH puncta observed within the VNC and resulted in a re-distribution of POSH to a more diffuse cytosolic localization (Fig. 2e-f). This was supported by our observation that overexpression of myrAKT was able to rescue reduced phosphorylation of POSH observed in lysates extracted from the VNC of *CHMP2B*^{Intron5} larvae (Supplementary Fig.1b).

Knockdown of POSH Alleviates *CHMP2B*^{Intron5} Toxicity in *Drosophila*

Having confirmed that POSH is a direct substrate of AKT and shown that AKT expression is sufficient to alleviate synaptic perturbations and aberrant localization of POSH in *CHMP2B*^{Intron5} expressing larvae, we asked whether POSH played a critical role in driving pathological pathways in *CHMP2B*^{Intron5} expressing animals. Using the *Drosophila* larval

NMJ as a model synapse we demonstrate knockdown of POSH via RNAi or using the previously characterized hypomorphic allele *POSH*^{74} (7, 29) was sufficient to alleviate all aspects of synaptic overgrowth observed in *CHMP2B*^{Intron5} expressing larvae, including increased synaptic bouton number and synapse length (Fig. 3a-c). Knockdown of POSH also alleviated impaired larval crawling in *CHMP2B*^{Intron5} expressing larvae (Fig. 3d).

In addition to neuroanatomical perturbations at the *Drosophila* larval NMJ pan-neuronal expression of *CHMP2B*^{Intron5} results in a 100% pharate (adult pupal) lethal phenotype. In order to ascertain whether inhibition of POSH could reduce the penetrance of this lethal phase, survival assays were performed. Experimental crosses were designed to give a 50:50 ratio of progeny either pan-neuronally expressing *CHMP2B*^{Intron5} or siblings not expressing *CHMP2B*^{Intron5} but carrying an identifiable marker (*CyO*, balancer chromosome with curly wings). The effect of reducing POSH expression, using both heterozygous and homozygous POSH mutants, on survival was then assessed in these backgrounds by scoring the number of flies with normal or curly wings eclosing as adults. A wild-type cross giving a 50:50 ratio of straight:curly winged flies was used as a baseline control. Pan-neuronal expression of *CHMP2B*^{Intron5} resulted in a 100% lethal phenotype, with all eclosing offspring carrying the *CyO* balancer (Fig 3e). In contrast, homozygous *POSH (POSH* $^{74/74}$*)* mutants pan-neuronally expressing *CHMP2B*^{Intron5} showed reduced lethality, with 40% of eclosing flies expressing the *CHMP2B*^{Intron5} transgene (Fig 3e).

Neuronal Accumulation of POSH Mediating Toxicity is Conserved in Mammalian Models of *CHMP2B*^{Intron5} FTD

Having observed aberrant accumulation of POSH within the nervous system of flies expressing *CHMP2B*^{Intron5} we asked whether this phenotype was conserved in mammalian CHMP2B^{Intron5} models. We therefore employed our previously established *CHMP2B*^{Intron5} mouse model(30). POSH accumulation was observed in β3-tubulin positive neurons within the frontal cortex of 12-month old mice expressing *CHMP2B*^{Intron5} but not aged matched *CHMP2B*$^{Wild\text{-}type}$ expressing controls (Fig.4). Accumulations were specific to the cell body and neuronal processes. Quantification of the relative fluorescence abundance of POSH within β3-tubulin positive neurons showed a significant increase in *CHMP2B*^{Intron5} expressing mice, compared to *CHMP2B*$^{Wild\text{-}type}$ controls. β3-tubulin expression showed no significant variance to wild-type.

Previously we demonstrated mammalian neurons transfected with *CHMP2B*^{Intron5} show dendritic collapse prior to death(13). Similar phenotypes are observed via knockdown of *CHMP2B*(31). In order to ascertain whether POSH plays a functional role in *CHMP2B*^{Intron5} toxicity in mammalian neurons, we asked whether knockdown of POSH via shRNA could alleviate dendritic collapse and convey neuroprotection (Fig.5). Neurons transfected with *CHMP2B*^{Intron5} showed a significant dendritic collapse phenotype compared to those transfected with wild-type *CHMP2B*. Sholl analysis revealed *CHMP2B*^{Intron5} transfected neurons show reduced complexity of the dendritic arbor, with a significant decrease in the number of cumulative intersections observed compared to neurons transfected CHMP2B$^{Wild\text{-}type}$ (Fig. 5a-b). *CHMP2B*^{Intron5} transfected neurons also showed a significant reduction in the length of the longest neuronal process (Fig. 5a&c, 56% reduction), the maximum number of intersections at any given distance from the cell body (Fig. 5a&d, 50% reduction) and the total arbor size (Fig. 5a&e, 66% reduction). The total perimeter of the cell body showed no variance between neurons transfected with either *CHMP2B*^{Intron5} or *CHMP2B*$^{Wild\text{-}type}$. Co-

transfection of *POSH* shRNA's was sufficient to alleviate all aspects of perturbed dendritic morphology associated with expression of *CHMP2B*^{Intron5} (Fig.5).

Knockdown of POSH Alleviates Elevated Apoptotic Cascades In *CHMP2B*^{Intron5} Models.

Previous studies have identified POSH as a pro-apoptotic JNK scaffold(15-17). Overexpression of POSH has been shown to induce neuronal apoptosis while knockdown conveys neuroprotection against ischemia(16, 23, 24). Having observed neuroprotection via knockdown of POSH in both *Drosophila* and mammalian models of *CHMP2B*^{Intron5} FTD, we asked whether expression of *CHMP2B*^{Intron5} resulted in elevated JNK and apoptotic activity in these models.

Pan-neuronal expression of *CHMP2B*^{Intron5} resulted in an increase in TUNEL staining observed in the *Drosophila* larval VNC (Fig. 6a), coupled with a significant increase in the expression of cleaved Death Caspase 1 (Dcp-1) (Fig. 6b-c), the activated *Drosophila* effector caspase(32). Immunoblotting revealed a 1.7 fold increase in cleaved Dcp-1 in the larval VNC, compared to wild-type (Fig. 6b) while immunofluorescence quantification of cleaved Dcp-1 specifically within elav positive neurons in the VNC revealed a 1.5 fold increase (Fig. 6c). Reduction of POSH abundance in flies expressing *CHMP2B*^{Intron5} using the hypomorphic POSH^{74} allele was sufficient to rescue cleaved Dcp-1 levels back to wild-type levels (Fig. 6b-c). Cleaved caspase 3 was also shown to be elevated in rat endothelial cells transfected with *CHMP2B*^{Intron5}, but not *CHMP2B*$^{Wild\text{-}type}$, supporting observations made in *Drosophila* (Fig. 6d). Inhibition of apoptosis using the deficiency allele Df(3L)H99, which has previously been shown to completely block apoptosis by deleting three essential pro-apoptotic genes(33),

acted to partially alleviate the *CHMP2B*^{Intron5} eye phenotype, reducing the severity of the black spot phenotype observed (Fig. 6e&f).

Having observed increased apoptotic activity in both *Drosophila* and mammalian models of *CHMP2B*^{Intron5} FTD, and taking into account the role of POSH as a pro-apoptotic JNK scaffold, we asked whether these models showed elevated JNK signalling and whether this could be alleviated by inhibition of POSH. Puckered (puc), a negative regulator of JNK transcriptionally activated by the JNK signaling pathway, has previously been shown to provide a reliable transcriptional readout of JNK activity(34, 35). Using a *puc*-lacZ reporter(34) we demonstrate a significant increase in JNK activity within the nervous system of *CHMP2B*^{Intron5} expressing larvae (Fig. 6g), supporting our previous observations(7). Inhibition of POSH was sufficient to alleviate elevated levels of *puc*. A significant increase in phospho-JNK was also observed in lysates extracted from the cortex of 12-month-old *CHMP2B*^{Intron5} expressing mice, compared to aged matched CHMP2B$^{Wild\text{-}type}$ expressing controls (Fig. 6h&i).

Discussion

As part of an ongoing, functional screen to identify signaling mechanisms driving pathology in FTD we identified AKT as a potent modifier of *CHMP2B*^{Intron5} toxicity. Expression of *CHMP2B*^{Intron5} lead to aberrant accumulation of POSH, which is known to be negatively regulated by AKT(18, 20), in the nervous system of both *Drosophila* and mammalian models. Having previously implicated POSH as a potential regulator of neuronal dysfunction(7) this study now defines, for the first time, the function of this novel regulator of apoptosis in an FTD model.

AKT in *CHMP2B*^{Intron5}-Associated FTD

AKT has been implicated in the regulation of neuronal growth and survival as well as conveying neuroprotection in response to neuronal insults(36-39). It has been identified as a potential therapeutic target for neuroprotective compounds in response to ischemia and neurotoxic apoptosis(40). Perturbations to AKT function have been implicated in a number of neurodegenerative disorders including Alzheimer's Disease and FTD(41-44). It has also been show to directly interact with a number of proteins associated with FTD disease causing loci, including TBK1 and VCP(45-47). In this study, we identified the single *Drosophila* isoform of AKT, to be a potent modifier of *CHMP2B*^{Intron5} toxicity. *AKT* loss-of-function mutants were shown to significantly enhance the eye phenotype associated with *CHMP2B*^{Intron5} expression, revealing heterozygous mutations of AKT to be dominant enhancers of *CHMP2B*^{Intron5} toxicity. The most significant enhancement to the eye phenotype was shown by the *AKT*^{1} allele, an endogenous kinase-dead allele(25). This observation suggests an important functional role for AKT kinase activity in preventing neurotoxicity associated with the *CHMP2B*^{Intron5} mutation. This is supported by the ability of both AKT and the constitutively active myristoylated AKT to rescue aberrant synaptic growth at the *Drosophila* larval NMJ, as well as impaired locomotor velocity. We also substantiate previous findings that POSH is a direct substrate of AKT and show that POSH aberrantly accumulates in the CNS of AKT kinase-dead flies. Despite this we did not observe changes in either AKT or pAKT levels in *CHMP2B*^{Intron5} models (data not shown). This suggests POSH accumulation in *CHMP2B*^{Intron5} does not occur as a result of perturbed pro-survival AKT function, but more likely in response to endogenous pro-apoptotic stimuli promoting assembly of the active POSH-complex. Activation of the pro-survival AKT pathway, however, is sufficient to alleviate POSH mediated toxicity, most likely through its known role as a negative regulator of POSH. This may therefore represent a pathway for therapeutic

intervention. Similarly, disruption to AKT kinase function may potentiate disease severity by reducing negative regulation of the POSH signaling complex.

Additionally, we have demonstrated that reducing *POSH* expression alleviates synaptic overgrowth both in *CHMP2B*^{Intron5} expressing flies and, previously, in *Rab8* mutants(7). Collectively this data reveals POSH as a novel candidate potentially acting downstream of AKT to modulate synaptic structural homeostasis. Given the known function of POSH as a JNK scaffold and the well-established role of the JNK-activator protein 1 (AP-1) pathway in regulating synaptic outgrowth at the *Drosophila* NMJ, POSH represents a promising candidate linking AKT to JNK-dependent regulation of NMJ morphology in an antagonistic manner. Given the conservation of AKT and JNK signaling pathways in neuronal growth and plasticity across species, observations made at the *Drosophila* larval NMJ may be directly translatable to a mammalian system and in the regulation of neuronal homeostasis in neuropathology(48, 49).

Modulation of POSH by AKT

Scaffolding proteins are post-translationally modified to modulate their activation state. AKT is as a negative regulator of the pro-apoptotic POSH-JNK signalling complex in the mammalian nervous system and in cell culture(18, 20). Negative regulation of this complex occurs through phosphorylation of POSH and its interacting partners(18-20). Direct phosphorylation of POSH by AKT, however, has previously only been shown *in vitro* or in cell culture(18). Here we provide evidence that POSH is an AKT substrate in the *Drosophila* nervous system and that inhibition of AKT kinase function leads to aberrant POSH accumulation. The observation that AKT expression alleviates POSH accumulation and toxicity in the nervous system of *CHMP2B*^{Intron5} expressing flies also provides context for this pathway in FTD. Identification of this pathway in the regulation of neuronal growth and

function in FTD model identifies the POSH signalling complex as a novel target mediating neuronal dysfunction and neurodegeneration in FTD.

Inhibition of POSH is Neuroprotective in *Drosophila* and Mammalian Models of *CHMP2B*^{Intron5} FTD

POSH has been implicated in the development and maintenance of the nervous system, including neuronal migration and axon outgrowth(50-52). POSH knockdown conveys neuroprotection in response to neuronal insults, suggesting an important role for POSH in the regulation and survival of neurons(16, 24). For example, knockdown of POSH is neuroprotective in response to cerebral ischemia and growth factor withdrawal(16, 24). Conversely, overexpression of POSH induces caspase-dependent cell death(53). AKT is also implicated in neuroprotection in response to ischemia and growth factor withdrawal, supporting a conserved mechanism in which modulation of POSH by AKT promotes neuroprotection in response to neuronal insults(36-39). Here we provide evidence that POSH knockdown is sufficient to alleviate neuronal perturbations in both *Drosophila* and mammalian models of FTD associated with the disease-causing *CHMP2B*^{Intron5} mutation. POSH knockdown in *Drosophila* pan-neuronally expressing *CHMP2B*^{Intron5} completely alleviated unregulated neuronal growth at the larval NMJ. Importantly POSH knockdown had no effect upon neuroanatomy in wild-type larvae suggesting a role for POSH in pathological neuronal dysfunction, rather than as a mediator of neuronal growth. POSH knockdown was also sufficient to ameliorate perturbed larval crawling and early-lethality observed in *CHMP2B*^{Intron5} flies, suggesting a pathological role for POSH leading to premature lethality in *Drosophila*. The observation that POSH knockdown ameliorated all aspects of the dendritic collapse phenotype observed in primary neurons transfected with *CHMPB*^{Intron5}

provides functional evidence for a conserved role of POSH in the transduction of neurotoxic pathways in both *Drosophila* and mammalian models of disease.

POSH as a pro-apoptotic JNK Scaffold in FTD

Premature apoptosis has been observed as an early event occurring in different FTD variants(1) and a number of FTD causing loci are implicated in neuronal apoptosis (VCP, TBK1, GRN)(8, 9). Activation of microglia has also been shown to promote clearance of apoptotic neurons observed in the brains of 18-month old *CHMP2B*^{Intron5} mice, but not aged matched *CHMP2B*$^{Wild\text{-}type}$ or non-transgenic controls, indicating aberrant neuronal apoptosis may be driving cell-loss in *CHMP2B*^{Intron5}-associated FTD(14). Mutations in *CHMP2B* have also been suggested to pre-dispose neurons to apoptosis(54). However, our understanding of whether apoptosis is driving cell death in FTD and the molecular machinery regulating this process remains poorly understood. Our observation that the pro-apoptotic JNK scaffold POSH aberrantly accumulates in both *Drosophila* and mammalian models of *CHMP2B*^{Intron5} FTD and that POSH knockdown alleviates aberrant neuronal phenotypes identifies it as a potentially novel pro-apoptotic factor in FTD pathology.

POSH was initially identified in the regulation of JNK and NF-κB dependent apoptosis(15). POSH overexpression promotes caspase-dependent cell death, while knockdown promotes neuroprotection following neuronal insult(16, 23, 24). Ablation of SH3RF2, a negative regulator of POSH, leads to enhanced caspase-8 activity(55). Conversely expression of SH3RF2 prevents apoptosis and promotes neuronal cell survival through inhibition of POSH(21, 55). The pro-apoptotic function of Nix/BNIP3L, has also been shown to be dependent upon interaction with POSH(56) . However, to date, POSH remains poorly studied and its role in neurodegenerative diseases remains unknown. This study is the first, to

our knowledge, providing a functional context for POSH in a neurodegenerative disorder. We provide evidence that inhibition of POSH alleviates elevated caspase activity in both *Drosophila* and mammalian *CHMP2B*^{Intron5}-induced FTD models. We also reveal inhibition of apoptosis using the *Df(3L)H99* deficiency locus, which ablates 3 essential apoptotic genes and reduces *CHMP2B*^{Intron5} toxicity as a heterozygote. However, it is important to note that the *Df(3L)H99 allele* does not completely alleviate the eye phenotype, suggesting a potential role for alternative pathways in *CHMP2B*^{Intron5} toxicity. These may include non-canonical cell death pathways as well as autophagic pathways, which are known to be perturbed in *CHMP2B*^{Intron5} models. Interestingly the *Drosophila* effector caspase Dcp-1 has also been implicated in autophagic flux(57). This may represent a broader link to other mechanisms of cell death and autophagic disruption in FTD.

Implications for FTD

In this study we provide evidence for a functional, novel, role for the pro-apoptotic JNK scaffold POSH in mediating neuropathology in *Drosophila* and mammalian models of FTD associated with the disease-causing mutation *CHMP2B*^{Intron5}. Aberrant apoptosis has been implicated as a potential mechanism driving neuronal cell death and gliosis in a number of FTD variants. The observation that POSH is perturbed in *CHMP2B*^{Intron5} models therefore raises the question of whether this novel apoptotic-regulator has a functional role in other variants of the disease, or even more broadly in neurodegenerative diseases. Future investigation into the role of POSH in FTD and other neurodegenerative diseases, as well as whether aberrant POSH accumulation is conserved in patients, will be critical to elucidate the role of POSH neurodegeneration. Further investigation into novel interacting partners of POSH in both healthy and diseased neurons may also help to delineate mechanisms regulating POSH and its downstream effects on neurodegeneration.

These observations provide the first characterization of POSH as a potential component of neuropathological cascades in FTD. It also reveals POSH as a novel target for further investigation and potential therapeutic intervention. Aberrant accumulation of POSH may also represent a biomarker of the disease though further investigation will be required to determine this.

Materials and Methods

Drosophila

Stocks and Husbandry:

Drosophila were raised on standard cornmeal-yeast-sucrose medium at 25°C on a 12h light:dark cycle. CHMP2B^{Intron5} flies were described previously (7, 10). All other stocks were obtained from the following sources: POSH^{74} (Toshiro Aigaki, Tokyo Metropolitan University, Japan) (29), AKT^{1} (Clive Wilson, University of Oxford, UK) (25), OK6-Gal4 (Cahir O'Kane, University of Cambridge, UK), UAS-myrAKT, UAS-mCD8-GFP, AKT^{04226}, AKT^{3}, UAS-AKT-RNAi (BL #33615), UAS-mCherry-POSH, UAS-POSH-RNAi (BL #64569), Df(3L)H99, Puc-LacZ, GMR-Gal4, nSyb-Gal4, Canton S, w^{1118}, (Bloomington Stock Center). UAS-AKT (FlyORF, Zurich, Switzerland). All wild-types were an outcross of Canton S to w^{1118}.

Genetic interaction experiments and quantification of the *CHMP2B^{Intron5}* eye phenotype was performed as described previously (7). Eyes were imaged using an AxioCam ERc 5s camera (Carl Zeiss) mounted on a Stemi 2000-C stereo microscope (Carl Zeiss).

Immunohistochemistry:

Drosophila Immunohistochemistry was performed as described previously(7). Primary antibodies used were: Cleaved Dcp-1 (Cell Signaling Technology, 9578, 1:100), HRP-Cy3 (Jackson scientific, Stratech), Synaptotagmin (1:2000)(7), β-galactosidase (1:1,000; MP Biologicals 0855976) and anti-elav (1:50, DSHB 9F8A9). All primary antibodies were incubated overnight at 4°C in PBS-T (0.1% Triton X-100), all secondary antibodies were incubated for 1h at room temp (~21°C) in PBS-T. Terminal Deoxynucleotidyl Transferase (TdT)-Mediated dUTP Nick-End Labeling (TUNEL) staining was performed using TMR-red detection kit (Roche, 12 156 792 910).

Imaging and Quantification:

Quantification of synaptic bouton number at the *Drosophila* third instar larval Neuromuscular Junction (NMJ) was performed as described previously (7). Confocal microscopy was performed using a Zeiss LSM 880 on an Axio Observer.Z1 invert confocal microscope (Zeiss). Z-stacked projections of NMJ's and VNCs were obtained using a Plan Neofluar 40x/0.75 NA oil objective. NMJ lengths were measured from stacked NMJ images using the NeuronJ plugin for ImageJ (National Institutes of Health) as described previously (7). Corrected total cell fluorescence quantification was performed as described previously using ImageJ (7). Neurons were identified in the *Drosophila* larval VNC using anti-elav.

Larval Locomotor Assay:

Female third instar wandering larvae of the appropriate genotype were selected and transferred into HL3 (70 mM NaCl, 5 mM KCl, 1 mM $CaCl_2.2H_2O$, 10 mM $NaHCO_3$, 5 mM trehalose, 115 mM sucrose and 5 mM BES in dH_2O) to wash off any debris. 2-3 larvae were transferred onto the center of a 90mm diameter petri-dish containing a thin layer of 1% agar and left to acclimatise. The petri dish was placed upon a black surface and imaged from

above using a digital webcam (Creative labs, UK). Experiments were performed at 25°C. Upon initiation of crawling larvae were recorded for 120 sec. (0.2 frames sec-1) using VirtualDub software. Images were analysed using imageJ. Briefly videos were batch thresholded and a custom macro used to track, via the MTrack2 plugin, and plot the larval positions. This data was then used to determine the mean larval velocity.

Mouse

Ex Vivo Histology:

Brains were isolated from 12 month aged CHMP2B$^{Wild\text{-}type}$ and CHMP2B^{Intron5} expressing mice, described previously (30), and fixed in 4% formalin for 24 hours. Tissue was embedded in paraffin blocks and 5 µm sagittal sections taken. Sections were deparaffinised by heating at 55°C for 10 mins followed by further xylene deparaffinisaton and rehydrated in a graded series of ethanol. Heat mediated antigen retrieval was performed in sodium citrate buffer (10 mM Sodium citrate, 0.05% Tween 20, pH 6.0, 95°C, 10 mins.) followed by Retrievagen (pH 6.0, 95°C, 10 mins. BD Biosciences). Samples were blocked in 5% Goat Serum (TBST 0.025%, 1h room temp.) followed by endogenous mouse IgG blocking (AffiniPure Fab Fragment Goat Anti-Mouse IgG (H+L), Jackson immune research, stratech). Samples were incubated in primary antibodies (POSH (1:100, Proteintech, 14649-1-AP) and β3 Tubulin (1:500, Sigma T-8660) 1% BSA, TBST 0.025%, overnight, 4°C) followed by secondary antibodies (goat anti-mouse FITC, goat anti-rabbit Cy3, 1h, room temperature, Jackson scientific, stratech). Samples were mounted in Vectashield mounting media + DAPI (H-1200, Vector labs) and analyzed using a Zeiss LSM 880 confocal (Plan Neofluar 40x/0.75 NA oil objective). Relative abundance of POSH within mouse cortical neurons was determined via corrected total cell fluorescence (CTCF) using ImageJ. Relative fluorescence

intensity of POSH was normalized against relative fluorescence intensity of β3-Tubulin. 3 – 5 cortical neurons per animal, 3 animals per genotype were analysed.

Cell Culture

Animal groups:

Timed mated female Wistar rats (Charles River UK) (RRID:RGD_737929) were maintained in accordance with the ARRIVE guidelines and the UK Animals (Scientific Procedures) Act (1986). Hippocampi were dissected from postnatal day 1-4 (P1-4) rat pups. Animals were euthanised using pentobarbital injection followed by cervical dislocation, according to Home Office guidelines. Hippocampal cell suspensions were obtained as previously described (Potter, 1989) and cultured in Neurobasal medium (21103049, Thermo Scientific) supplemented with B27 (50x, 17504044, Thermo Scientific), Glucose (35mM final concentration, A2494001, Thermo Scientific), L-glutamine (1mM, 25030032, Thermo Scientific), Foetal Calf Serum (5%, Mycoplex, PAA), Penicillin (100u/ml) and Steptomycin (100µg/ml, 15140122, Thermo Scientific) and maintained at 37°C in 5% CO_2.

Neurons were transfected at 12 days *in vitro* (DIV) with Lipofectamine 2000 (11668019, Thermo Scientific) with either FLAG-tagged *CHMP2B*$^{wild\text{-}type}$ or *CHMP2B*^{Intron5}, described previously (13), and with POSH ShRNA 1+2 or Scrambled ShRNA's (52) (supplementary Fig. 1c). After 2/3 days, cells were fixed or lysed for biochemical experiments. GPNT's (Sigma) were cultured in Ham's F-10 (Lonza, BE12-618F) with L-Glutamine supplemented with basic fibroblast growth factor (FGF, 2ng/ml, Sigma F3685), heparin (80µg/ml, Sigma H3149) and Foetal Calf Serum (10%). Cells were plated in 35mm dishes and at ~70% confluency transfected with either 20µg CHMP2B$^{Wild\text{-}type}$ or CHMP2B^{Intron5}. After 3 DIV, cells were lysed for western blotting. Culture media was routinely screened for mycoplasma contamination.

Immunocytochemistry:

Cells were washed with phosphate buffered saline (PBS) and fixed for 30 min at room temperature with 4% paraformaldehyde (containing 4% sucrose) (Sigma) PBS. Cells were permeabilized in 0.5% NP40 in PBS for 5 minutes at room temperature. Primary antibodies used were as follows: anti-FLAG (Sigma M2 clone, 1:1000), anti-GFP (eBioscience, 14-6758-81, 1:1000). dsRed was detected using FluoTag-X4, ATTO 542 (1:500, Synaptic Systems). Primary antibodies were incubated overnight at 4°C. Corresponding Alexafluor secondary antibodies (1:500, Thermo Scientific) were incubated for 1 hour at room temperature before mounting with Fluoromount (Sigma).

Microscopy and Image Analysis:

Images were collected on an inverted Zeiss microscope (880) with 20x or 63x Plan Neofluar objectives using Zeiss filter sets for DAPI and Alexa 488/546/633. Images were taken at an aspect ratio of 2048x2048. Images of neurons were traced using the NeuronJ plugin in ImageJ (1.6.0). Individual traces were saved, thresholded and sholl analysis was conducted using the Sholl plugin.

Biochemistry

Western Blotting:

7 brains, per genotype, were dissected from third instar wandering larvae and boiled in 20µl of 2x laemmli loading buffer. Cells were lysed in RIPA containing phosSTOP phosphatase inhibitors (Roche) and cOmplete EDTA free protease inhibitors (Roche). Cortical lysates were extracted from mouse brain as described previously (30). After boiling in loading buffer samples were run on a 4–20% Mini-PROTEAN® TGX™ Precast Protein Gels (Biorad) prior to transfer onto standard PVDF membrane. Antibodies used for immunoblotting were Guinea

Pig Anti-POSH (193, 1:5000), anti-Phospho-(Ser/Thr) Akt Substrate (Cell signaling Technology, 9611, 1:1000), anti-Cleaved Dcp-1 (Cell Signaling Technology 9578, 1:1000), anti-β-Actin (Proteintech, 60008-1-Ig (7D2C10), 1:180 000), anti-Cleaved Caspase 3 (CC3) (1:200, Cell Signaling Technology 9661), anti-GAPDH (Merck, MAB374 (6C5), 1:10,000), anti-pJNK (Promega Active JNK, pTPpY, 1:5000) and anti-Pan-JNK (Cell Signaling Technology 9252 1:1000). Secondary antibodies were Peroxidase-conjugated AffiniPure Goat Anti-Guinea Pig, anti-rabbit and anti-mouse IgG (H+L) (Jackson Scientific, 106-035-003, 111-035-144 and 115-035-003, 1:10 000). For immunoblotting following immunoprecipitation secondary antibodies were Peroxidase-conjugated protein-G (Merck Millipore 18-161, 1:10 000). POSH antibodies were produced from full length GST-tagged *Drosophila* POSH, generated from POSH cDNA (LD45365, Berkeley Drosophila Genome Project Gold Collection) and injected into Rabbit or Guinea Pig (eurogentec, 87-day immunization). Phospho mobility shift gels were performed by addition of Phos-tag acrylamide (AAL-107, Wako laboratory chemicals) to standard acrylamide gels as per the manufacturer's instructions.

Immunoprecipitation:

For immunoprecipitation protein was extracted from *Drosophila* in RIPA containing phosSTOP phosphatase inhibitors (Roche) and cOmplete EDTA free protease inhibitors (Roche). Lysates were incubated at a concentration of 1mg/ml with Rabbit Anti-POSH (429, 4°C, overnight)) followed by incubation with protein A-agarose beads (Sigma, P2545, 4°C, 4 hours). Following incubation Protein A-agarose beads were collected using a Spin-X tube filter (Corning, Costar, 0.45µm), washed and the sample eluted in 2x laemmli. Western blotting was performed as described above.

Statistics:

Statistical analysis was performed using either SPSS Statistics (IBM, Version 24) or GraphPad Prism (6.01). Data are presented as mean values, from at least 3 biological replicates, with error bars representing the standard error of mean (S.E.M). Mean, S.E.M, statistical tests, P-values and sample sizes are reported in the figure legends.

Acknowledgements

We thank Hongru Zhou for mouse tissue collection. We also thank Toshiro Aigaki (Tokyo Metropolitan University, Japan), Zhiheng Xu (Chinese Academy of Sciences, Beijing, China), Clive Wilson (University of Oxford, UK), Cahir O'Kane (University of Cambridge, UK), The Bloomington *Drosophila* Stock Center (Indiana, USA) and The Zurich ORFeome Project (Zurich, Switzerland) for providing *Drosophila* stocks and reagents. We thank the University of York Technology Facility for providing access to confocal microscopes.

Funding

We thank the Alzheimer's Society UK [AS-PG-2013-005 to S.T.S]; Alzheimer's Research UK [ARUK-PPG2017A-7 to S.T.S]; the Medical Research Council [MR/M013596/1 to S.T.S]; and The National Institutes of Health (NIH) (NS057553 to F.B.G) for funding this work.

Conflict of Interest

All authors declare no competing financial interests of conflicts of interest.

References

1 Broe, M., Kril, J. and Halliday, G.M. (2004) Astrocytic degeneration relates to the severity of disease in frontotemporal dementia. *Brain*, **127**, 2214-2220.

2 Ferrari, R., Forabosco, P., Vandrovcova, J., Botia, J.A., Guelfi, S., Warren, J.D., Consortium, U.K.B.E., Momeni, P., Weale, M.E., Ryten, M. *et al.* (2016) Frontotemporal dementia: insights into the biological underpinnings of disease through gene co-expression network analysis. *Mol. Neurodegener.*, **11**, 21.

3 Ferrari, R., Hernandez, D.G., Nalls, M.A., Rohrer, J.D., Ramasamy, A., Kwok, J.B., Dobson-Stone, C., Brooks, W.S., Schofield, P.R., Halliday, G.M. *et al.* (2014) Frontotemporal dementia and its subtypes: a genome-wide association study. *Lancet Neurol.*, **13**, 686-699.

4 Lui, H., Zhang, J., Makinson, S.R., Cahill, M.K., Kelley, K.W., Huang, H.Y., Shang, Y., Oldham, M.C., Martens, L.H., Gao, F. *et al.* (2016) Progranulin Deficiency Promotes Circuit-Specific Synaptic Pruning by Microglia via Complement Activation. *Cell*, **165**, 921-935.

5 Sjogren, M., Folkesson, S., Blennow, K. and Tarkowski, E. (2004) Increased intrathecal inflammatory activity in frontotemporal dementia: pathophysiological implications. *J. Neurol. Neurosurg. Psychiatry*, **75**, 1107-1111.

6 Su, J.H., Nichol, K.E., Sitch, T., Sheu, P., Chubb, C., Miller, B.L., Tomaselli, K.J., Kim, R.C. and Cotman, C.W. (2000) DNA damage and activated caspase-3 expression in neurons and astrocytes: evidence for apoptosis in frontotemporal dementia. *Exp. Neurol.*, **163**, 9-19.

7 West, R.J., Lu, Y., Marie, B., Gao, F.B. and Sweeney, S.T. (2015) Rab8, POSH, and TAK1 regulate synaptic growth in a Drosophila model of frontotemporal dementia. *J. Cell Biol.*, **208**, 931-947.

8 Li, M., Liu, Y., Xia, F., Wu, Z., Deng, L., Jiang, R. and Guo, F.J. (2014) Progranulin is required for proper ER stress response and inhibits ER stress-mediated apoptosis through TNFR2. *Cell. Signal.*, **26**, 1539-1548.

9 Vandermoere, F., El Yazidi-Belkoura, I., Slomianny, C., Demont, Y., Bidaux, G., Adriaenssens, E., Lemoine, J. and Hondermarck, H. (2006) The valosin-containing protein (VCP) is a target of Akt signaling required for cell survival. *J. Biol. Chem.*, **281**, 14307-14313.

10 Ahmad, S.T., Sweeney, S.T., Lee, J.A., Sweeney, N.T. and Gao, F.B. (2009) Genetic screen identifies serpin5 as a regulator of the toll pathway and CHMP2B toxicity associated with frontotemporal dementia. *Proc. Natl. Acad. Sci. U. S. A.*, **106**, 12168-12173.

11 Lu, Y., Zhang, Z., Sun, D., Sweeney, S.T. and Gao, F.B. (2013) Syntaxin 13, a genetic modifier of mutant CHMP2B in frontotemporal dementia, is required for autophagosome maturation. *Mol. Cell*, **52**, 264-271.

12 Skibinski, G., Parkinson, N.J., Brown, J.M., Chakrabarti, L., Lloyd, S.L., Hummerich, H., Nielsen, J.E., Hodges, J.R., Spillantini, M.G., Thusgaard, T. *et al.* (2005) Mutations in the endosomal ESCRTIII-complex subunit CHMP2B in frontotemporal dementia. *Nat. Genet.*, **37**, 806-808.

13 Lee, J.A., Beigneux, A., Ahmad, S.T., Young, S.G. and Gao, F.B. (2007) ESCRT-III dysfunction causes autophagosome accumulation and neurodegeneration. *Curr. Biol.*, **17**, 1561-1567.

14 Clayton, E.L., Mancuso, R., Nielsen, T.T., Mizielinska, S., Holmes, H., Powell, N., Norona, F., Larsen, J.O., Milioto, C., Wilson, K.M. *et al.* (2017) Early microgliosis precedes neuronal loss and behavioural impairment in mice with a frontotemporal dementia-causing CHMP2B mutation. *Hum. Mol. Genet.*, **26**, 873-887.

15 Tapon, N., Nagata, K., Lamarche, N. and Hall, A. (1998) A new rac target POSH is an SH3-containing scaffold protein involved in the JNK and NF-kappaB signalling pathways. *EMBO J.*, **17**, 1395-1404.
16 Xu, Z., Kukekov, N.V. and Greene, L.A. (2003) POSH acts as a scaffold for a multiprotein complex that mediates JNK activation in apoptosis. *EMBO J.*, **22**, 252-261.
17 Xu, Z., Kukekov, N.V. and Greene, L.A. (2005) Regulation of apoptotic c-Jun N-terminal kinase signaling by a stabilization-based feed-forward loop. *Mol. Cell. Biol.*, **25**, 9949-9959.
18 Lyons, T.R., Thorburn, J., Ryan, P.W., Thorburn, A., Anderson, S.M. and Kassenbrock, C.K. (2007) Regulation of the Pro-apoptotic scaffolding protein POSH by Akt. *J. Biol. Chem.*, **282**, 21987-21997.
19 Zhang, Q.G., Han, D., Xu, J., Lv, Q., Wang, R., Yin, X.H., Xu, T.L. and Zhang, G.Y. (2006) Ischemic preconditioning negatively regulates plenty of SH3s-mixed lineage kinase 3-Rac1 complex and c-Jun N-terminal kinase 3 signaling via activation of Akt. *Neuroscience*, **143**, 431-444.
20 Figueroa, C., Tarras, S., Taylor, J. and Vojtek, A.B. (2003) Akt2 negatively regulates assembly of the POSH-MLK-JNK signaling complex. *J. Biol. Chem.*, **278**, 47922-47927.
21 Wilhelm, M., Kukekov, N.V., Schmit, T.L., Biagas, K.V., Sproul, A.A., Gire, S., Maes, M.E., Xu, Z. and Greene, L.A. (2012) Sh3rf2/POSHER protein promotes cell survival by ring-mediated proteasomal degradation of the c-Jun N-terminal kinase scaffold POSH (Plenty of SH3s) protein. *J. Biol. Chem.*, **287**, 2247-2256.
22 Wang, C., Tao, Y., Wang, Y. and Xu, Z. (2010) Regulation of the protein stability of POSH and MLK family. *Protein Cell*, **1**, 871-878.
23 Zhang, M., Zhang, Y. and Xu, Z. (2010) POSH is involved in Eiger-Basket (TNF-JNK) signaling and embryogenesis in Drosophila. *J Genet Genomics*, **37**, 605-619.
24 Zhang, Q.G., Wang, R.M., Yin, X.H., Pan, J., Xu, T.L. and Zhang, G.Y. (2005) Knock-down of POSH expression is neuroprotective through down-regulating activation of the MLK3-MKK4-JNK pathway following cerebral ischaemia in the rat hippocampal CA1 subfield. *J. Neurochem.*, **95**, 784-795.
25 Staveley, B.E., Ruel, L., Jin, J., Stambolic, V., Mastronardi, F.G., Heitzler, P., Woodgett, J.R. and Manoukian, A.S. (1998) Genetic analysis of protein kinase B (AKT) in Drosophila. *Curr. Biol.*, **8**, 599-602.
26 Pilli, M., Arko-Mensah, J., Ponpuak, M., Roberts, E., Master, S., Mandell, M.A., Dupont, N., Ornatowski, W., Jiang, S., Bradfute, S.B. *et al.* (2012) TBK-1 promotes autophagy-mediated antimicrobial defense by controlling autophagosome maturation. *Immunity*, **37**, 223-234.
27 Ciura, S., Sellier, C., Campanari, M.L., Charlet-Berguerand, N. and Kabashi, E. (2016) The most prevalent genetic cause of ALS-FTD, C9orf72 synergizes the toxicity of ATXN2 intermediate polyglutamine repeats through the autophagy pathway. *Autophagy*, in press., 0.
28 Corbier, C. and Sellier, C. (2016) C9ORF72 is a GDP/GTP exchange factor for Rab8 and Rab39 and regulates autophagy. *Small GTPases*, in press., 1-6.
29 Tsuda, M., Langmann, C., Harden, N. and Aigaki, T. (2005) The RING-finger scaffold protein Plenty of SH3s targets TAK1 to control immunity signalling in Drosophila. *EMBO Rep*, **6**, 1082-1087.
30 Gascon, E., Lynch, K., Ruan, H., Almeida, S., Verheyden, J.M., Seeley, W.W., Dickson, D.W., Petrucelli, L., Sun, D., Jiao, J. *et al.* (2014) Alterations in microRNA-124 and AMPA

receptors contribute to social behavioral deficits in frontotemporal dementia. *Nat. Med.*, **20**, 1444-1451.
31 Chassefeyre, R., Martinez-Hernandez, J., Bertaso, F., Bouquier, N., Blot, B., Laporte, M., Fraboulet, S., Coute, Y., Devoy, A., Isaacs, A.M. *et al.* (2015) Regulation of postsynaptic function by the dementia-related ESCRT-III subunit CHMP2B. *J. Neurosci.*, **35**, 3155-3173.
32 Song, Z., McCall, K. and Steller, H. (1997) DCP-1, a Drosophila cell death protease essential for development. *Science*, **275**, 536-540.
33 Cashio, P., Lee, T.V. and Bergmann, A. (2005) Genetic control of programmed cell death in Drosophila melanogaster. *Semin. Cell Dev. Biol.*, **16**, 225-235.
34 Martin-Blanco, E., Gampel, A., Ring, J., Virdee, K., Kirov, N., Tolkovsky, A.M. and Martinez-Arias, A. (1998) puckered encodes a phosphatase that mediates a feedback loop regulating JNK activity during dorsal closure in Drosophila. *Genes Dev.*, **12**, 557-570.
35 Wu, H., Wang, M.C. and Bohmann, D. (2009) JNK protects Drosophila from oxidative stress by trancriptionally activating autophagy. *Mech. Dev.*, **126**, 624-637.
36 Gao, X., Zhang, H., Steinberg, G. and Zhao, H. (2010) The Akt pathway is involved in rapid ischemic tolerance in focal ischemia in Rats. *Transl Stroke Res*, **1**, 202-209.
37 Zhu, H., Zhang, Y., Shi, Z., Lu, D., Li, T., Ding, Y., Ruan, Y. and Xu, A. (2016) The Neuroprotection of Liraglutide Against Ischaemia-induced Apoptosis through the Activation of the PI3K/AKT and MAPK Pathways. *Sci. Rep.*, **6**, 26859.
38 Ahn, J.Y. (2014) Neuroprotection signaling of nuclear akt in neuronal cells. *Exp. Neurobiol.*, **23**, 200-206.
39 Brunet, A., Datta, S.R. and Greenberg, M.E. (2001) Transcription-dependent and -independent control of neuronal survival by the PI3K-Akt signaling pathway. *Curr. Opin. Neurobiol.*, **11**, 297-305.
40 Fukunaga, K. and Kawano, T. (2003) Akt is a molecular target for signal transduction therapy in brain ischemic insult. *J. Pharmacol. Sci.*, **92**, 317-327.
41 Chu, J., Lauretti, E. and Pratico, D. (2017) Caspase-3-dependent cleavage of Akt modulates tau phosphorylation via GSK3beta kinase: implications for Alzheimer's disease. *Mol. Psychiatry*, **22**, 1002-1008.
42 Kleinberger, G., Wils, H., Ponsaerts, P., Joris, G., Timmermans, J.P., Van Broeckhoven, C. and Kumar-Singh, S. (2010) Increased caspase activation and decreased TDP-43 solubility in progranulin knockout cortical cultures. *J. Neurochem.*, **115**, 735-747.
43 Lee, H.K., Kumar, P., Fu, Q., Rosen, K.M. and Querfurth, H.W. (2009) The insulin/Akt signaling pathway is targeted by intracellular beta-amyloid. *Mol. Biol. Cell*, **20**, 1533-1544.
44 Stopford, M.J., Higginbottom, A., Hautbergue, G.M., Cooper-Knock, J., Mulcahy, P.J., De Vos, K.J., Renton, A.E., Pliner, H., Calvo, A., Chio, A. *et al.* (2017) C9ORF72 hexanucleotide repeat exerts toxicity in a stable, inducible motor neuronal cell model, which is rescued by partial depletion of Pten. *Hum. Mol. Genet.*, **26**, 1133-1145.
45 Freischmidt, A., Wieland, T., Richter, B., Ruf, W., Schaeffer, V., Muller, K., Marroquin, N., Nordin, F., Hubers, A., Weydt, P. *et al.* (2015) Haploinsufficiency of TBK1 causes familial ALS and fronto-temporal dementia. *Nat. Neurosci.*, **18**, 631-636.
46 Ou, Y.H., Torres, M., Ram, R., Formstecher, E., Roland, C., Cheng, T., Brekken, R., Wurz, R., Tasker, A., Polverino, T. *et al.* (2011) TBK1 directly engages Akt/PKB survival signaling to support oncogenic transformation. *Mol. Cell*, **41**, 458-470.
47 Watts, G.D., Wymer, J., Kovach, M.J., Mehta, S.G., Mumm, S., Darvish, D., Pestronk, A., Whyte, M.P. and Kimonis, V.E. (2004) Inclusion body myopathy associated with Paget

disease of bone and frontotemporal dementia is caused by mutant valosin-containing protein. *Nat. Genet.*, **36**, 377-381.
48 Chimnaronk, S., Sitthiroongruang, J., Srisucharitpanit, K., Srisaisup, M., Ketterman, A.J. and Boonserm, P. (2015) The crystal structure of JNK from Drosophila melanogaster reveals an evolutionarily conserved topology with that of mammalian JNK proteins. *BMC Struct. Biol.*, **15**, 17.
49 Scanga, S.E., Ruel, L., Binari, R.C., Snow, B., Stambolic, V., Bouchard, D., Peters, M., Calvieri, B., Mak, T.W., Woodgett, J.R. *et al.* (2000) The conserved PI3'K/PTEN/Akt signaling pathway regulates both cell size and survival in Drosophila. *Oncogene*, **19**, 3971-3977.
50 Dickson, H.M., Zurawski, J., Zhang, H., Turner, D.L. and Vojtek, A.B. (2010) POSH is an intracellular signal transducer for the axon outgrowth inhibitor Nogo66. *J. Neurosci.*, **30**, 13319-13325.
51 Taylor, J., Chung, K.H., Figueroa, C., Zurawski, J., Dickson, H.M., Brace, E.J., Avery, A.W., Turner, D.L. and Vojtek, A.B. (2008) The scaffold protein POSH regulates axon outgrowth. *Mol. Biol. Cell*, **19**, 5181-5192.
52 Yang, T., Sun, Y., Zhang, F., Zhu, Y., Shi, L., Li, H. and Xu, Z. (2012) POSH localizes activated Rac1 to control the formation of cytoplasmic dilation of the leading process and neuronal migration. *Cell Rep*, **2**, 640-651.
53 Lennox, A.L. and Stronach, B. (2010) POSH misexpression induces caspase-dependent cell death in Drosophila. *Dev. Dyn.*, **239**, 651-664.
54 Cox, L.E., Ferraiuolo, L., Goodall, E.F., Heath, P.R., Higginbottom, A., Mortiboys, H., Hollinger, H.C., Hartley, J.A., Brockington, A., Burness, C.E. *et al.* (2010) Mutations in CHMP2B in lower motor neuron predominant amyotrophic lateral sclerosis (ALS). *PLoS One*, **5**, e9872.
55 Kim, T.W., Kang, Y.K., Park, Z.Y., Kim, Y.H., Hong, S.W., Oh, S.J., Sohn, H.A., Yang, S.J., Jang, Y.J., Lee, D.C. *et al.* (2014) SH3RF2 functions as an oncogene by mediating PAK4 protein stability. *Carcinogenesis*, **35**, 624-634.
56 Wilhelm, M., Xu, Z., Kukekov, N.V., Gire, S. and Greene, L.A. (2007) Proapoptotic Nix activates the JNK pathway by interacting with POSH and mediates death in a Parkinson disease model. *J. Biol. Chem.*, **282**, 1288-1295.
57 DeVorkin, L., Go, N.E., Hou, Y.C., Moradian, A., Morin, G.B. and Gorski, S.M. (2014) The Drosophila effector caspase Dcp-1 regulates mitochondrial dynamics and autophagic flux via SesB. *J. Cell Biol.*, **205**, 477-492.

Figure Legends

Fig.1

AKT is a dominant modifier of *CHMP2B*^{Intron5}. **a** Representative images showing dominant enhancement of the *Drosophila* eye phenotype, associated with expression of the FTD disease-causing *CHMP2B*^{Intron5} transgene in the *Drosophila* eye (GMR-Gal4), by AKT knockdown (RNAi), loss-of-function alleles (AKT^{04226} and AKT^{3}) and the AKT kinase-dead allele (AKT^{1}). **b** Quantification of the eye phenotype. **c – e** Co-expression of AKT or constitutively active myrAKT alleviates increased mean normalised synaptic bouton number (**d**) and NMJ length (**e**) at the *Drosophila* third instar larval neuromuscular junction (hemi-segment A3, muscle 6/7) in animals pan-neuronally (nSyb-Gal4) expressing the *CHMP2B*^{Intron5} transgene. NMJ's were analyzed across a minimum of 5 animals. One-way ANOVA with Dunnett's post-hoc comparison to wild-type controls (* $p < .05$, *** $p < .001$) and Tukey between groups comparison (# $p < .05$, ## $p < 0.01$ and ### $p < 0.001$). **f** Reduced locomotor velocity observed in larvae pan-neuronally (nSyb-Gal4) expressing *CHMP2B*^{Intron5} is ameliorated by co-expression of AKT or myrAKT. One-way ANOVA with Dunnett's post-hoc comparison to wild-type controls (*** $p < .001$) and Tukey between groups comparison (### $p < .001$). Scale bars = 10 μm. Error bars represent S.E.M, sample size is reported above each bar.

Fig. 2

AKT, a negative regulator of POSH, alleviates aberrant accumulation of POSH in the nervous system of *Drosophila* expressing the disease-causing *CHMP2B*^{Intron5} transgene. **a-b** pan-neuronal (nSyb-Gal4) expression of the *CHMP2B*^{Intron5} mutant transgene results in a significant accumulation of mCherry-POSH positive puncta throughout the ventral nerve cord of third instar *Drosophila* larvae (student's t-test *** $p < .001$). Aberrant accumulation of POSH puncta was also observed in the ventral nerve cord of flies expressing

CHMP2B^{Intron5} within motor neurons (OK6-Gal4) (**c**) and in AKT kinase-dead (AKT^{1}) larvae (student's t-test *** p < .001) (**d-e**). **f-g** co-expression of AKT significantly reduces the number of POSH positive accumulations observed in the ventral nerve cord of larvae pan-neuronally (nSyb-Gal4) expressing the *CHMP2B*^{Intron5} mutant transgene. One-way ANOVA with Dunnett's post-hoc comparison to wild-type controls (*** p < .001) and Tukey between groups comparison (### p < .001). Scale bars = 10 μm. Error bars represent S.E.M, sample size is reported above each bar.

Fig. 3

POSH knockdown alleviates *CHMP2B*^{Intron5} phenotypes in *Drosophila.* **a-c** Knockdown of POSH via POSH-RNAi or using the strong hypomorphic allele POSH^{74} rescues the increased mean normalized synaptic bouton number (**b**) and mean normalized NMJ length **(c)** observed in larvae pan-neuornally (nSyb-Gal4) expressing the *CHMP2B*^{Intron5} mutant transgene (muscle 6/7, hemi-segment A3). NMJ analysis was performed across a minimum of 5 individual animals. One-way ANOVA with Dunnett's post-hoc comparison to wild-type controls (* p < .05, *** p < .001) and Tukey between groups comparison (## p < .01, ### p < .001). Scale bars = 10 μm. **d** Knockdown of POSH ameliorates impaired larval locomotion in larvae pan-neuronally (nSyb-Gal4) expressing the *CHMP2B*^{Intron5} mutant transgene. One-way ANOVA with Dunnett's post-hoc comparison to wild-type controls (* p < .05, ** p < .01, *** p < .001) and Tukey between groups comparison (# p < .05, ## p < .01). **e** pan-neuronal expression of the *CHMP2B*^{Intron5} mutant transgene results in a 100% pharate (pupal) lethal phenotype which can be ameliorated by knockdown of POSH using a homozygous POSH^{74} hypomorphic allele (POSH$^{74/74}$). Error bars represent S.E.M, sample size is reported above each bar.

Fig. 4

Aberrant neuronal accumulation of POSH is conserved in *CHMP2B*^{Intron5} mice

a-d representative images and quantification, via corrected total cell fluorescence (CTCF), of POSH within beta 3 tubulin positive neurons in the frontal cortex of 12 month old mice expressing either *CHMP2B*^{Intron5} or CHMP2B^{Wiltype} under the control of the Camk2a promoter. d. Relative fluorescence intensity of POSH (c) was normalized against relative fluorescence intensity of beta 3 tubulin (b). Student's t-test ** $p < .01$, *** $p < .001$. n = 12, N = 3. Scale bars = 10 μm. Error bars represent S.E.M.

Fig. 5

POSH knockdown alleviates *CHMP2B*^{Intron5} dependent dendritic collapse in mammalian neurons. **a** Representative micrographs of mature neurons expressing FLAG-tagged *CHMP2B*$^{Wild\text{-}type}$ or *CHMP2B*^{Intron5} in the presence of either pSIREN-RetroQ-DsRed-Scrambled or POSH 1+2 shRNA. Scale bars = 20μm. **b-e** *CHMP2B*^{Intron5} shows significant reduction in cumulative branch number (compared to *CHMP2B*$^{Wild\text{-}type}$ + Scrambled ($p < .001$) and *CHMP2B*^{Intron5} + POSH shRNA's ($p < .001$)) (**b**), longest process length (**c**) maximum number of dendritic branches (**d**) and total arbor size (**e**) without affecting cell body size (**f**). **c-f** One-way ANOVA with Dunnett's post-hoc comparison to wild-type controls (*** $p < .001$) and Tukey between groups comparison (# $p < .05$, ## $p < .01$ and ## $p < .001$) n = 30 cells across three biological replicates. Error bars represent S.E.M, sample size is reported above each bar.

Fig. 6

POSH knockdown alleviates aberrant apoptotic and JNK Activity in *Drosophila* and mammalian *CHMP2B*^{Intron5} models. Pan-neuronal (nSyb-Gal4) expression of *CHMP2B*^{Intron5} leads to an increase in apoptotic markers in the *Drosophila* third instar larval nervous system, including an increase in TUNEL (**a**) and cleaved Dcp-1, the *Drosophila* effector caspase, in the larval ventral nerve cord (**b-c**). Neuronal expression of *CHMP2B*^{Intron5} also resulted in an increase in the apoptosis related 50 kDa band recognized by anti-Dcp-1 via immunoblotting (**b**). CTCF = corrected total cell fluorescence. Knockdown of POSH using the hypomorphic POSH^{74} allele ameliorates elevated cleaved Dcp-1 in animals expressing *CHMP2B*^{Intron5} (**b-c**). One-way ANOVA with Dunnett's post-hoc comparison to wild-type controls (*** $p < .001$) and Tukey between groups comparison (## $p < .01$). **d** Immunoblot showing cleaved-caspase 3 (CC3) in mammalian GPNT cells transfected with *CHMP2B*$^{Wild\text{-}type}$ and *CHMP2B*^{Intron5}. **e-f** The deficiency locus Df(3L)H99, which ablates three critical apoptotic loci, reduces the *CHMP2B*^{Intron5} eye phenotype (GMR-Gal4). **g – i** *Drosophila* and mouse models expressing *CHMP2B*^{Intron5} show elevated levels of JNK activity within the nervous system. Elevated JNK activity, determined using the transcriptional reporter puckered-lacZ, in the ventral nerve cord of *Drosophila* third instar larvae pan-neuronally expressing *CHMP2B*^{Intron5} (nSyb-Gal4) can be alleviated by POSH knockdown using the hypomorphic POSH^{74} allele (**g**). pJNK levels in cortical lysates extracted from 12 month old mice expressing either *CHMP2B*^{Intron5} or *CHMP2B*^{Wiltype} under the control of the Camk2a promoter (**h**) and quantified relative to the actin loading control (**i**, N = 3. (student's t-test *** $p < .001$). Error bars represent S.E.M, sample size is reported above each bar.

Figure S1.

POSH is a substrate of AKT. **a** Immunoblot probed using the anti-phospho-(Ser/Thr) Akt substrate antibody following immunoprecipitation of POSH from *Drosophila* third instar

larval lysates. **b** Phos-tag mobility shift assay demonstrating a reduction in the phosphorylation of POSH (asterisk) in larvae pan-neuronally (nSyb-Gal4) expressing *CHMP2B*^{Intron5} and amelioration by co-expression of myrAKT. **c** Immunoblot showing POSH-shRNA knockdown efficiency in GPNT cells.

Abbreviations

FTD: Frontotemporal Dementia

POSH: Plenty of SH3s

SH3RF1: SH3 Domain Containing Ring Finger 1

CHMP2B: Charged Multivesicular Body Protein 2B

JNK: Jun N-terminal Kinase

FTLD: Frontotemporal lobar degeneration

bvFTD: behavioral variant FTD

FTD-MND: FTD with Motor Neuron Disease

VCP: Valosin Containing Protein

TBK1: TANK Binding Kinase 1

GRN: Granulin Precursor

RNAi: RNA interference

shRNA: Short hairpin RNA

nSyb: Neuronal Synaptobrevin

UAS: Upstream activator sequence

myrAKT: myristoylated AKT

pAKT: Phospho-AKT

NMJ: Neuromuscular Junction

MND: Motor Neuron Disease

VNC: Ventral nerve cord

Dcp-1: Death Caspase 1

Puc: Puckered

CNS: central nervous system

AP-1: activator protein 1

SH3RF2: SH3 Domain Containing Ring Finger 2

HRP: horseradish peroxidase

TUNEL: Terminal Deoxynucleotidyl Transferase (TdT)-Mediated dUTP Nick-End Labeling

CyO: curly of oster

GMR: Glass multimer reporter

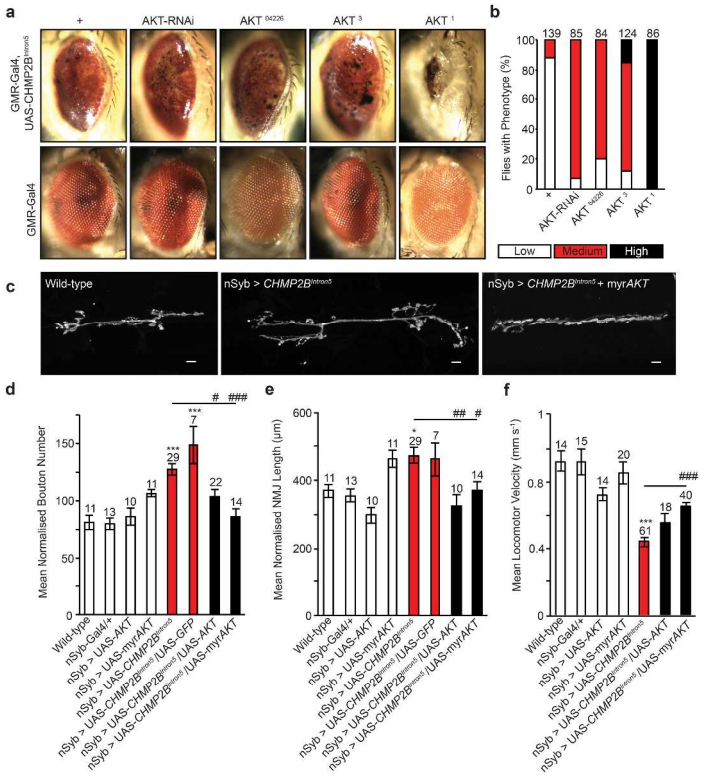

Fig.1 AKT is a dominant modifier of CHMP2B^{Intron5}. **a** Representative images showing dominant enhancement of the Drosophila eye phenotype, associated with expression of the FTD disease-causing CHMP2B^{Intron5} transgene in the *Drosophila* eye (GMR-Gal4), by AKT knockdown (RNAi), loss-of-function alleles (AKT^{04226} and AKT^{3}) and the AKT kinase-dead allele (AKT1). **b** Quantification of the eye phenotype. **c – e** Co-expression of AKT or constitutively active myrAKT alleviates increased mean normalised synaptic bouton number (**d**) and NMJ length (**e**) at the Drosophila third instar larval neuromuscular junction (hemi-segment A3, muscle 6/7) in animals pan-neuronally (nSyb-Gal4) expressing the CHMP2BIntron5 transgene. NMJ's were analyzed across a minimum of 5 animals. One-way ANOVA with Dunnett's post-hoc comparison to wild-type controls (* $p < .05$, *** $p < .001$) and Tukey between groups comparison (# $p < .05$, ## $p < 0.01$ and ### $p < 0.001$). **f** Reduced locomotor velocity observed in larvae pan-neuronally (nSyb-Gal4) expressing CHMP2BIntron5 is ameliorated by co-expression of AKT or myrAKT. One-way ANOVA with Dunnett's post-hoc comparison to wild-type controls (*** $p < .001$) and Tukey between groups comparison (### $p < .001$). Scale bars = 10 µm. Error bars represent S.E.M, sample size is reported above each bar.

297x420mm (300 x 300 DPI)

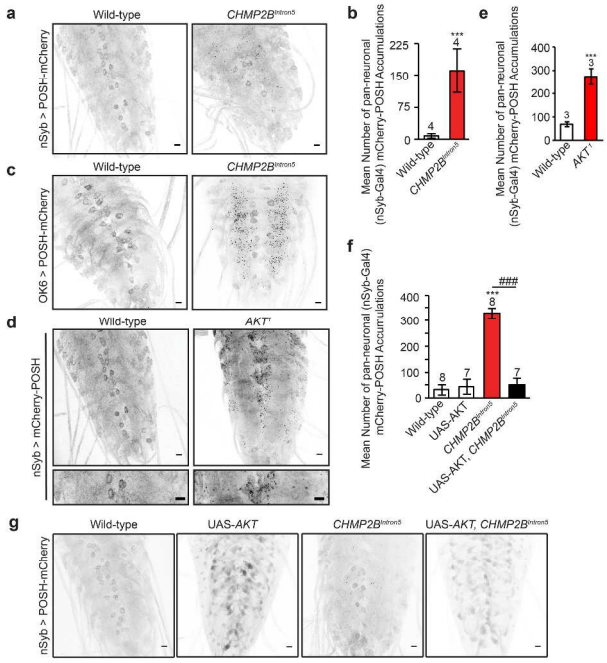

Fig. 2 ‼ ┼ AKT, a negative regulator of POSH, alleviates aberrant accumulation of POSH in the nervous system of *Drosophila* expressing the disease-causing CHMP2B^{Intron5} transgene. **a-b** pan-neuronal (nSyb-Gal4) expression of the CHMP2B^{Intron5} mutant transgene results in a significant accumulation of mCherry-POSH positive puncta throughout the ventral nerve cord of third instar *Drosophila* larvae (student's t-test *** $p < .001$). Aberrant accumulation of POSH puncta was also observed in the ventral nerve cord of flies expressing CHMP2B^{Intron5} within motor neurons (OK6-Gal4) (**c**) and in AKT kinase-dead (AKT^{1}) larvae (student's t-test *** $p < .001$) (**d-e**). **f-g** co-expression of AKT significantly reduces the number of POSH positive accumulations observed in the ventral nerve cord of larvae pan-neuronally (nSyb-Gal4) expressing the CHMP2B^{Intron5}mutant transgene. One-way ANOVA with Dunnett's post-hoc comparison to wild-type controls (*** $p < .001$) and Tukey between groups comparison (### $p < .001$). Scale bars = 10 μm. Error bars represent S.E.M, sample size is reported above each bar.

297x420mm (300 x 300 DPI)

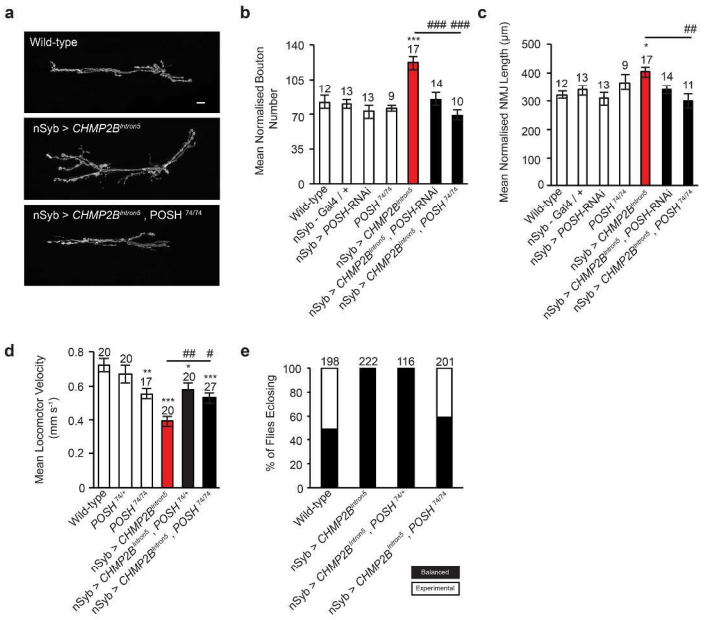

Fig. 3

POSH knockdown alleviates CHMP2B^{Intron5} phenotypes in *Drosophila*. **a-c** Knockdown of POSH via POSH-RNAi or using the strong hypomorphic allele POSH^{74} rescues the increased mean normalized synaptic bouton number (**b**) and mean normalized NMJ length (**c**) observed in larvae pan-neuornally (nSyb-Gal4) expressing the CHMP2B^{Intron5} mutant transgene (muscle 6/7, hemi-segment A3). NMJ analysis was performed across a minimum of 5 individual animals. One-way ANOVA with Dunnett's post-hoc comparison to wild-type controls (* $p < .05$, *** $p < .001$) and Tukey between groups comparison (## $p < .01$, ### $p < .001$). Scale bars = 10 µm. **d**. Knockdown of POSH ameliorates impaired larval locomotion in larvae pan-neuronally (nSyb-Gal4) expressing the CHMP2B^{Intron5} mutant transgene. One-way ANOVA with Dunnett's post-hoc comparison to wild-type controls (* $p < .05$, ** $p < .01$, *** $p < .001$) and Tukey between groups comparison (# $p < .05$, ## $p < .01$). **e** pan-neuronal expression of the CHMP2B^{Intron5} mutant transgene results in a 100% pharate (pupal) lethal phenotype which can be ameliorated by knockdown of POSH using a homozygous POSH^{74} hypomorphic allele (POSH$^{74/74}$). Error bars represent S.E.M, sample size is reported above each bar.

297x420mm (300 x 300 DPI)

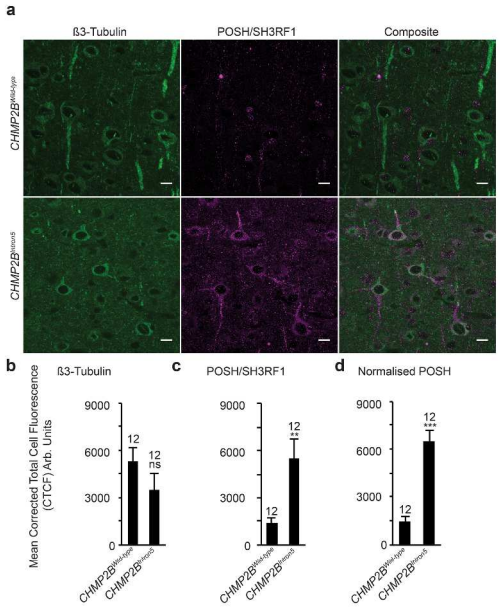

Fig. 4 ‼ ┼ Aberrant neuronal accumulation of POSH is conserved in CHMP2B^{Intron5} mice‼ ┼ **a-d** representative images and quantification, via corrected total cell fluorescence (CTCF), of POSH within beta 3 tubulin positive neurons in the frontal cortex of 12 month old mice expressing either CHMP2B^{Intron5} or CHMP2B^{Wiltype} under the control of the Camk2a promoter. **d.** Relative fluorescence intensity of POSH (**c**) was normalized against relative fluorescence intensity of beta 3 tubulin (**b**). Student's t-test ** p < .01, *** p < .001. n = 12, N = 3. Scale bars = 10 μm. Error bars represent S.E.M.‼ ┼

297x420mm (300 x 300 DPI)

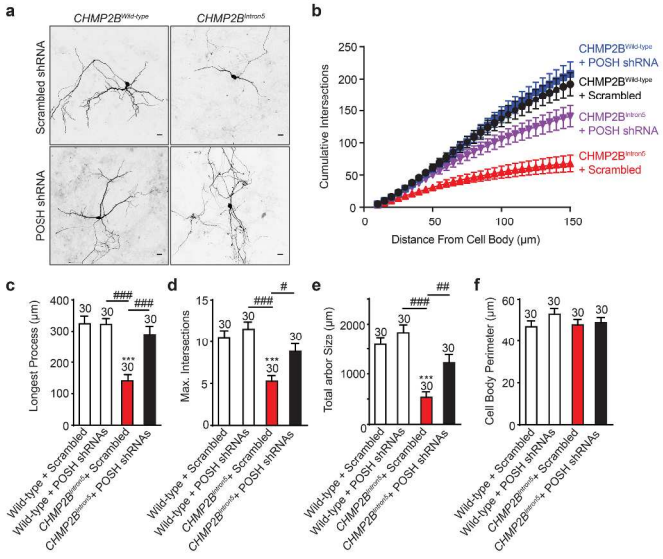

Fig. 5

POSH knockdown alleviates CHMP2B^{Intron5} dependent dendritic collapse in mammalian neurons. **a** Representative micrographs of mature neurons expressing FLAG-tagged CHMP2B$^{Wild\text{-}type}$ or CHMP2B^{Intron5} in the presence of either pSIREN-RetroQ-DsRed-Scrambled or POSH 1+2 shRNA. Scale bars = 20μm. **b-e** CHMP2B^{Intron5} shows significant reduction in cumulative branch number (compared to CHMP2B$^{Wild\text{-}type}$ + Scrambled ($p < .001$) and CHMP2B^{Intron5} + POSH shRNA's ($p < .001$)) (**b**), longest process length (**c**) maximum number of dendritic branches (**d**) and total arbor size (**e**) without affecting cell body size (**f**). **c-f** One-way ANOVA with Dunnett's post-hoc comparison to wild-type controls (*** $p < .001$) and Tukey between groups comparison (# $p < .05$, ## $p < .01$ and ## $p < .001$) n = 30 cells across three biological replicates. Error bars represent S.E.M, sample size is reported above each bar.

297x420mm (300 x 300 DPI)

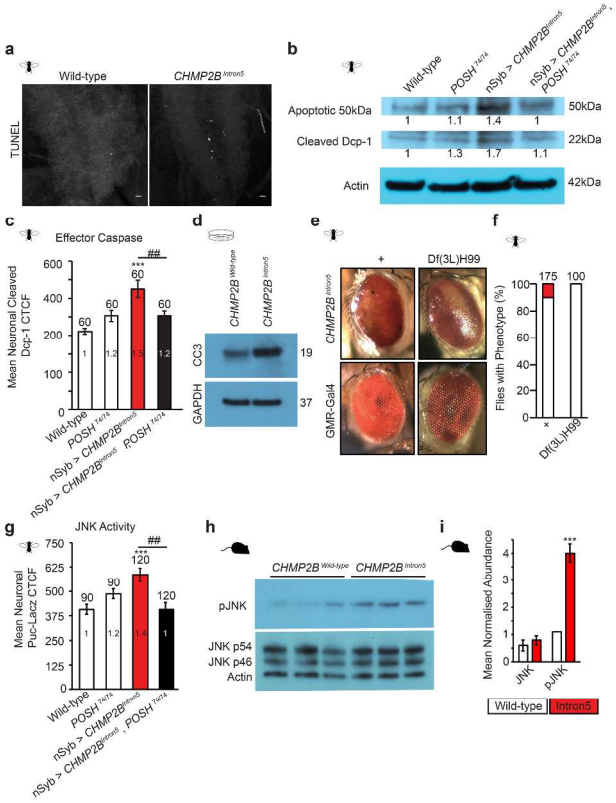

Fig. 6

POSH knockdown alleviates aberrant apoptotic and JNK Activity in *Drosophila* and mammalian CHMP2B^{Intron5} models. Pan-neuronal (nSyb-Gal4) expression of CHMP2B^{Intron5} leads to an increase in apoptotic markers in the *Drosophila* third instar larval nervous system, including an increase in TUNEL (**a**) and cleaved Dcp-1, the *Drosophila* effector caspase, in the larval ventral nerve cord (**b-c**). Neuronal expression of CHMP2B^{Intron5} also resulted in an increase in the apoptosis related 50 kDa band recognized by anti-Dcp-1 via immunoblotting (**b**). CTCF = corrected total cell fluorescence. Knockdown of POSH using the hypomorphic POSH^{74} allele ameliorates elevated cleaved Dcp-1 in animals expressing CHMP2B^{Intron5} (**b-c**). One-way ANOVA with Dunnett's post-hoc comparison to wild-type controls (*** $p < .001$) and Tukey between groups comparison (## $p < .01$). **d** Immunoblot showing cleaved-caspase 3 (CC3) in mammalian GPNT cells transfected with CHMP2B$^{Wild-type}$ and CHMP2B^{Intron5}. **e-f** The deficiency locus Df(3L)H99, which ablates three critical apoptotic loci, reduces the CHMP2B^{Intron5} eye phenotype (GMR-Gal4). **g – i** *Drosophila* and mouse models expressing CHMP2B^{Intron5} show elevated levels of JNK activity within the nervous system. Elevated JNK activity,

determined using the transcriptional reporter puckered-lacZ, in the ventral nerve cord of *Drosophila* third instar larvae pan-neuronally expressing $CHMP2B^{Intron5}$ (nSyb-Gal4) can be alleviated by POSH knockdown using the hypomorphic $POSH^{74}$ allele (**g**). pJNK levels in cortical lysates extracted from 12 month old mice expressing either $CHMP2B^{Intron5}$ or $CHMP2B^{Wiltype}$ under the control of the Camk2a promoter (h) and quantified relative to the actin loading control (i, N = 3. (student's t-test *** $p < .001$). Error bars represent S.E.M, sample size is reported above each bar.

297x420mm (300 x 300 DPI)